Photoluminescence properties of single Mn-doped CdS nanocrystals studied by scanning near-field optical microscopy

Atsushi Ishizumi
Graduate School of Materials Science, Nara Institute of Science and Technology, Ikoma, Nara 630-0192, Japan

Kazunari Matsuda[a] and Toshiharu Saiki[b]
Kanagawa Academy of Science and Technology, Takatsu, Kawasaki 213-0012, Japan

C. W. White
Condensed Matter Sciences Division, Oak Ridge National Laboratory, Oak Ridge, Tennessee 37831

Yoshihiko Kanemitsu[c]
Institute for Chemical Research, Kyoto University, Uji, Kyoto 611-0011, Japan

(Received 20 May 2005; accepted 3 August 2005; published online 20 September 2005)

We have fabricated Mn-doped CdS (CdS:Mn) nanocrystals embedded in Al_2O_3 matrices by sequential ion implantation and studied their photoluminescence (PL) properties by a scanning near-field optical microscope (SNOM). In the PL spectra of CdS:Mn nanocrystals measured by the SNOM, several sharp PL lines and a broad PL band were observed. The sharp PL lines are related to bound excitons at shallow impurities in CdS nanocrystals. The Mn-related PL spectrum is very broad even in single nanocrystals at low temperatures, and both the peak energy and the spectral width of the PL band depend on the excitation laser intensity. The PL properties of single CdS:Mn nanocrystals are discussed. © *2005 American Institute of Physics*. [DOI: 10.1063/1.2058228]

In the past decade, there have been many studies of the fabrication and optical properties of semiconductor nanocrystals doped with luminescence centers, because they exhibit efficient luminescence even at room temperature.[1] Chemical synthesis methods are usually used for the fabrication of nanocrystals doped with luminescence centers.[2–4] However, it is pointed out that almost doped ions are located near the nanocrystal surface,[5,6] and the luminescence properties of impurity-doped nanocrystals depend on the surface structure and the surrounding chemical environment.[3] The development of new routes of the fabrication of impurity-doped semiconductor nanocrystals is important and needed in the research field of semiconductor nanocrystals.

Very recently, it has been demonstrated that ion implantation is one of the most versatile methods for the fabrication of compound semiconductor nanocrystals embedded in transparent matrices.[7–9] In this method, impurity-doped semiconductor nanocrystals can be simply fabricated by sequential ion implantation of the elements forming compound semiconductors and impurities. For example, Mn-doped CdS (Ref. 10) and Cu- and Al-codoped ZnS nanocrystals[11] have been fabricated by sequential ion implantation followed by thermal annealing. Efficient photoluminescence (PL) is observed in these impurity-doped nanocrystal samples. The detailed studies of the impurity-related PL are important for the understanding of the nature of impurity states in nanocrystals and new functionalities of impurity-doped nanocrystals.

In this work, we have studied impurity-related PL properties of Mn-doped CdS (CdS:Mn) nanocrystals at low temperatures by means of a scanning near-field optical microscope (SNOM). In the spatially resolved PL spectra of CdS:Mn nanocrystals, both sharp PL lines and a broad PL band were observed. The sharp PL lines are assigned to bound excitons at shallow impurities. The broad PL band is caused by the intra-3*d* transition of Mn^{2+} ions in single CdS nanocrystals. The PL properties of single CdS:Mn nanocrystals are discussed.

CdS:Mn nanocrystals were fabricated by ion implantation of Cd^+ (4.5×10^{16} cm^{-2} at 430 keV), S^+ (4.5×10^{16} cm^{-2} at 157 keV), and Mn^+ (2.0×10^{14} cm^{-2} at 250 keV) into the *c*-axis-oriented single crystal α-Al_2O_3 substrate, and then the samples were annealed at 1000 °C for 60 min in flowing 96% Ar+4% H_2 atmosphere. The average size of hexagonal CdS:Mn nanocrystals is evaluated to be ~17 nm.[10]

The spatially resolved PL spectra were measured by means of a SNOM operated at low temperatures. For the measurements of the near-field PL, the sample was illuminated with 405 nm light (laser diode) through an aperture of a fiber probe. The PL signals from the sample were collected by the same aperture (a so-called illumination and collection mode).[12] The diameter of the fiber aperture was about 200 nm. The spectra of the near-field PL were measured by a cooled charge-coupled device detector through a 32 cm monochromator. In addition, the conventional far-field PL spectra were measured under 325 nm He–Cd laser light excitation, and were detected by a photomultiplier tube through a 25 cm monochromator. A gated photon counting method (chopping frequency: 330 Hz, gate width: 1.4 ms) was used for the measurement of the Mn-related PL with a long lifetime and the elimination of the surface-defect PL of CdS nanocrystals. We measured the far-field PL spectra at 405 and 325 nm excitation wavelengths. There is no significant

[a]Also at Institute for Chemical Research, Kyoto University, Uji, Kyoto 611-0011, Japan and Nanostructure and Material Property, PRESTO, Japan Science and Technology Agency, 4-1-8 Honcho, Saitama 332-0012, Japan.
[b]Also at Department of Electronics and Electrical Engineering, Keio University, 3-14-1 Hiyoshi, Kohoku, Yokohama, Kanagawa 223-8522, Japan.
[c]Author to whom correspondence should be addressed; electronic mail: kanemitu@scl.kyoto-u.ac.jp

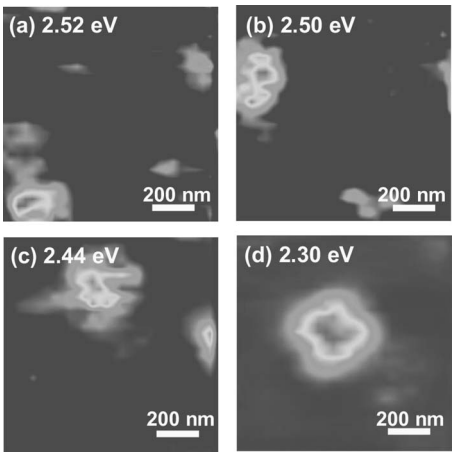

FIG. 1. (Color online) Spatial PL images at the energies of (a) 2.52, (b) 2.50, (c) 2.44, and (d) 2.30 eV at 10 K.

difference in the PL spectra at these excitation wavelengths. The spectral sensitivity of the measuring system was calibrated using a tungsten standard lamp.

Figure 1 shows near-field images monitored at different PL energies at 10 K: (a) 2.52 (b) 2.50, (c) 2.44, and (d) 2.30 eV. The 1 μm$\times$1 μm images of Fig. 1 consist of 30 $\times$30 points with $\sim$33 nm separations between the points due to the scanning steps. The PL spectra were measured at all the points. The bright spots in the images correspond to the PL signals of single CdS:Mn nanocrystals. The diameter of the bright spots is estimated to be about 200 nm from the full width at half-maximum (FWHM) of the cross sectional intensity profile of the PL signal. The luminescent spot size is determined mainly by the aperture size of the fiber probe used in this work.

Figure 2 shows near-field PL spectra at the bright spots. The near-field PL spectra of Figs. 2(a)–2(d) were measured at the luminescent positions in Figs. 1(a)–1(d), respectively. In Figs. 2(a)–2(c), sharp PL lines are observed at 2.52, 2.50, and 2.44 eV, respectively. From the images, we can see that the peak energy of the sharp PL line is very sensitive to the monitored position. The sharp PL lines were also observed in the near-field PL spectra of nondoped CdS nanocrystals embedded in Al_2O_3 matrices. It is concluded that these PL lines are related to shallow impurities of CdS nanocrystals.[13]

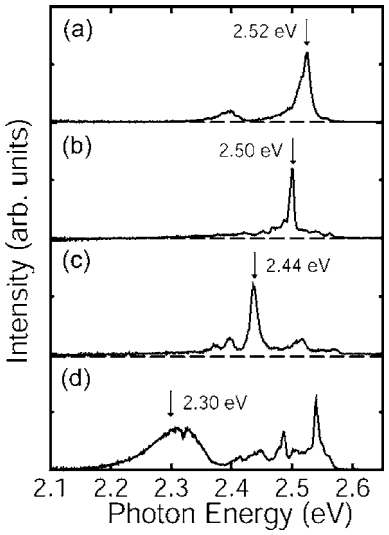

FIG. 2. (a)–(d) Near-field PL spectra at bright spots shown in Figs. 1(a)–1(d), respectively, under 405 nm excitation at 10 K.

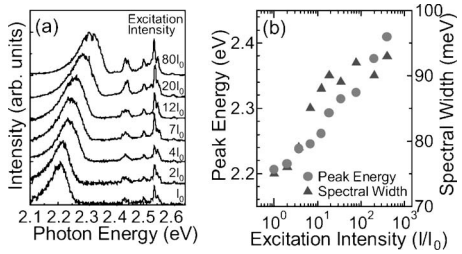

FIG. 3. (Color online) (a) Near-field PL spectra at different excitation intensities under 405 nm excitation at 10 K. (b) Excitation intensity dependence of the peak energy and the spectral width of the Mn-related PL band in single CdS:Mn nanocrystals.

In Fig. 2(d), a broad PL band is also observed around 2.30 eV, in addition to the sharp PL lines. This broad PL band was not observed in the near-field PL spectra of nondoped CdS nanocrystals in this energy range. Therefore, we can assign that the broad band does not come from an assembly of sharp PL lines due to shallow impurities, but from Mn^{2+}-related PL band of individual nanocrystals. The validity of this assignment is also supported from the longer decay time of millisecond order of the broad PL band, as will be described later. In the PL spectra of Figs. 2(a)–2(c), we cannot observe the Mn-related broad PL band. It is concluded that there exist nondoped and Mn-doped CdS nanocrystals in our samples.

At the luminescent position in Fig. 1(d), the excitation intensity dependence of the near-field PL was measured at 10 K. Figure 3(a) shows near-field PL spectra as a function of the excitation laser intensity. Here, the excitation intensity I_0 is estimated to be $\sim$1 W/cm^2 from the laser intensity coupled to the fiber probe and the size of the aperture. The peak energy and the linewidth of the sharp PL lines do not change. This implies that the laser-induced thermal effects (temperature rise) and many-particle effects of electron-hole pairs[14] can be negligible under our experimental condition. On the other hand, the peak energy and spectral width of the broad Mn-related PL band depend strongly on the excitation laser intensity. The peak energy and spectral width of the broad PL band are plotted as a function of the excitation intensity in Fig. 3(b). With a decrease of the excitation intensity, the PL peak energy shifts to the lower energy and the PL spectral width (FWHM) decreases. In the near-field PL spectrum shown in Fig. 2(d), the Mn-related PL spectrum appears around 2.30 eV, because the near-field images and spectra in Figs. 1 and 2 were measured under $\sim 30 I_0$ excitation intensity. These intensity dependences were not clearly observed in the far-field PL spectra. The near-field PL measurements are useful for the study of the broad impurity PL.

Figure 4(a) shows a near-field PL spectrum under the lowest excitation intensity (I_0) in this experiment. In addition, Figs. 4(b) and 4(c) show time-integrated far-field PL and time-gated far-field PL (chopping frequency: 330 Hz, gate width: 1.4 ms) spectra, respectively. The time-gated far-field PL shows that the lifetime of the Mn^{2+}-related PL band is on the order of ms. In Fig. 4(b), the broad PL band around 2.45 eV is related to bound excitons at shallow impurities in CdS nanocrystals; this consists of assembly of sharp PL lines of individual CdS:Mn nanocrystals. Under the weak excitation, the peak energy of the Mn-related PL in the near-field

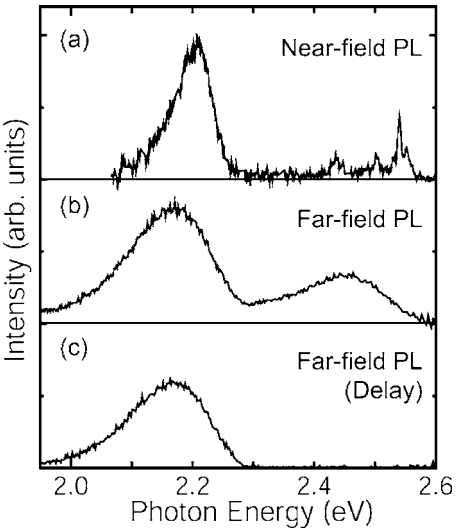

FIG. 4. (a) The near-field PL spectrum under weak 405 nm excitation at 10 K. (b) The spectrum of the far-field PL under 325 nm excitation at 14 K. (c) The spectrum of the delay component of the far-field PL measured by a gated photon counting method (chopping frequency: 330 Hz, gate width: 1.4 ms) under 325 nm excitation at 14 K.

PL spectrum almost coincides with that in the far-field PL spectrum. However, the spectral width (FWHM) of the near-field PL spectrum (about 80 meV) is much narrower than that of the far-field PL spectrum (about 160 meV). The Mn^{2+}-related PL spectrum in our samples is broadened by the inhomogeneous distribution of the transition energy of Mn^{2+} ions, in addition to the homogeneous broadening by the strong electron-phonon coupling (a phonon side band of the $^4T_1$-$^6A_1$ transition of Mn^{2+} ions).[15]

Here, we discuss the intensity dependence of the Mn-related PL spectrum in single CdS nanocrystals. The intensity-dependent PL spectrum suggests that a single CdS:Mn nanocrystal contains many Mn^{2+} ions in our sample and there is an inhomogeneous distribution of the Mn^{2+} transition energy in single nanocrystals. It is well known that the energy of intra-3*d* transition of Mn^{2+} ions depends strongly on the crystal field around the Mn^{2+} ions.[16] The surrounding-environment-sensitive $^4T_1$-$^6A_1$ transition energy in Mn^{2+} ions causes the broad and intensity-dependent PL spectrum. Under high intensity excitation, many Mn^{2+} ions are excited in single nanocrystals and the broadening of the spectral width occurs. Under weak laser excitation, the Mn^{2+} ions with the lower transition energy mainly contribute to the PL processes, because of energy transfer between Mn^{2+} ions.[17] The excitation intensity dependence of the Mn-related PL band can be first observed by using a SNOM technique, because the spectral widths of the Mn^{2+}-related and shallow-impurity PL bands in the near-field PL are much narrower than those in the far-field PL. The spatially resolved PL measurements are useful for the understanding of the impurity states in semiconductor nanocrystals.

In conclusion, we have studied the PL properties of single CdS:Mn nanocrystals fabricated by sequential ion implantation using a SNOM technique. The spatially resolved PL spectra show that there exist Mn-doped and undoped CdS nanocrystals in the samples. The blueshift of the PL peak and the spectral broadening of the PL band occur with an increase of the excitation laser intensity. It is pointed out that the intensity dependence of the PL spectrum is caused by energy transfer between Mn^{2+} ions within individual nanocrystals. The spatially resolved PL spectroscopy is one of the most useful methods for characterization of impurity-doped nanocrystals embedded in transparent matrices.

Part of this work was supported by The Research Foundation of Opto-Science and Technology and The Futaba Electronics Memorial Foundation. Oak Ridge National Laboratory is managed by UT-Battelle, LLC for the U.S. Department of Energy under Contract No. DE-AC05-00OR22725.

[1] See, for example, L. E. Brus, Al. L. Efros, and T. Itoh, J. Lumin. **70**, 1 (1996).
[2] R. N. Bhargava, D. Gallagher, X. Hong, and A. Nurmikko, Phys. Rev. Lett. **72**, 416 (1994).
[3] A. A. Bol and A. Meijerink, Phys. Rev. B **58**, R15997 (1998); Phys. Status Solidi B **224**, 291 (2001).
[4] M. Tanaka, J. Lumin. **100**, 163 (2002).
[5] G. Counio, T. Gacoin, and J. P. Boilot, J. Phys. Chem. B **102**, 5257 (1998).
[6] H. Yang and P. H. Holloway, Appl. Phys. Lett. **82**, 1965 (2003).
[7] C. W. White, J. D. Budai, S. P. Withrow, J. G. Zhu, E. Sonder, R. A. Zuhr, A. Meldrum, D. M. Hembree, Jr., D. O. Henderson, and S. Prawer, Nucl. Instrum. Methods Phys. Res. B **141**, 228 (1998).
[8] Y. Kanemitsu, H. Tanaka, T. Kushida, K. S. Min, and H. A. Atwater, Phys. Rev. B **62**, 5100 (2000).
[9] D. Matsuura, Y. Kanemitsu, T. Kushida, C. W. White, J. D. Budai, and A. Meldrum, Appl. Phys. Lett. **77**, 2289 (2000).
[10] Y. Kanemitsu, H. Matsubara, and C. W. White, Appl. Phys. Lett. **81**, 535 (2002).
[11] A. Ishizumi, C. W. White, and Y. Kanemitsu, Appl. Phys. Lett. **84**, 2397 (2004).
[12] T. Saiki and K. Matsuda, Appl. Phys. Lett. **74**, 2773 (1999).
[13] M. Ando, Y. Kanemitsu, T. Kushida, K. Matsuda, T. Saiki, and C. W. White, Appl. Phys. Lett. **79**, 539 (2001).
[14] Y. Kanemitsu, T. J. Inagaki, M. Ando, K. Matsuda, T. Saiki, and C. W. White, Appl. Phys. Lett. **81**, 141 (2002).
[15] D. Langer and S. Ibuki, Phys. Rev. **138**, A809 (1965).
[16] *Phosphor Handbook*, edited by S. Shionoya and W. M. Yen (CRC Press, Boca Raton, FL, 1999).
[17] S. Yamamoto, K. Takamura, and J. Nakahara, Phys. Status Solidi B **211**, 111 (1999).